DMD Fast Forward. Published on June 22, 2011 as doi:10.1124/dmd.111.039065

DMD #39065

Evaluation of CYP2C8 Inhibition *In Vitro*:

Utility of Montelukast as a Selective CYP2C8 Probe Substrate

Brooke M. VandenBrink, Robert S. Foti, Dan A. Rock, Larry C. Wienkers and Jan L. Wahlstrom*

Pharmacokinetics and Drug Metabolism, Amgen, Inc, Seattle, WA 98119

Running title:

Evaluation of CYP2C8 Probe Substrates

Corresponding author:

*To whom correspondence should be addressed:
Jan L Wahlstrom
Pharmacokinetics and Drug Metabolism
Amgen, Inc
1201 Amgen Court West
Mail Stop AW2/D2262
Seattle, WA 98119
Phone: (206)265-7423
FAX: (206)217-0494
janw@amgen.com

Manuscript metrics:

Text pages: 22

Tables: 3

Figures: 6

References: 36

Words in the abstract: 221

Words in the introduction: 703

Words in the results and discussion: 2,254

Abbreviations:

DDIs, drug-drug interactions; FMO, flavin-containing monooxygenase; HPLC, high-performance liquid chromatography; LC-MS/MS, liquid chromatography/tandem mass spectrometry; P450, cytochrome P450

Abstract

Understanding the potential for cytochrome P450 mediated drug-drug interactions is a critical step in the drug discovery process. While *in vitro* studies with CYP3A4, CYP2C9 and CYP2C19 have suggested the presence of multiple binding regions within the P450 active site based upon probe substrate-dependent inhibition profiles, similar studies have not been carried out with CYP2C8. The ability to understand CYP2C8 probe substrate sensitivity will enable appropriate *in vitro* and *in vivo* probe selection. In order to characterize the potential for probe substrate-dependent inhibition with CYP2C8, the inhibition potency of twenty-two known inhibitors of CYP2C8 were measured *in vitro* using four clinically relevant CYP2C8 probe substrates (montelukast, paclitaxel, repaglinide and rosiglitazone) and amodiaquine. Repaglinide exhibited the highest sensitivity to inhibition *in vitro*. *In vitro* phenotyping indicated that montelukast is an appropriate probe for CYP2C8 inhibition studies. The *in vivo* sensitivities of the CYP2C8 probe substrates cerivastatin, fluvastatin, montelukast, pioglitazone and rosiglitazone were determined in relation to repaglinide based upon clinical DDI data. Repaglinide exhibited the highest sensitivity *in vivo*, followed by cerivastatin, montelukast and pioglitazone. Finally, the magnitude of *in vivo* CYP2C8 DDI caused by gemfibrozil-1-*O*-β-glucoronide was predicted. Comparisons of the predictions with clinical data coupled with the potential liabilities of other CYP2C8 probes suggest that montelukast is an appropriate CYP2C8 probe substrate to use for the *in vivo* situation.

DMD Fast Forward. Published on June 22, 2011 as DOI: 10.1124/dmd.111.039065
This article has not been copyedited and formatted. The final version may differ from this version.

Introduction

The cytochrome P450 (P450) superfamily of drug metabolizing enzymes is involved in the metabolism of a majority of currently prescribed drugs and new chemical entities (Wienkers and Heath, 2005). Within the P450 superfamily, CYP2C8 is responsible for 5-8% of P450-mediated metabolism and is involved in the metabolism of over 60 drugs, including antimalarials (amodiaquine), antidiabetics (pioglitazone, repaglinide and rosiglitazone), statins (cerivastatin and fluvastatin) and anticancer agents (paclitaxel) (Lai et al., 2009). Due to the general importance of CYP2C8 in drug clearance, assessment of probe substrate dependence on CYP2C8 inhibition is a key part of the drug discovery and development process (Wahlstrom et al., 2006). The overall goal of studying CYP2C8 probe substrate-dependent inhibition is to gain a comprehensive understanding of *in vitro* and *in vivo* sensitivity, which will enable appropriate probe substrate selection.

The *in vitro* marker reactions recommended by the U.S. Food and Drug Administration (FDA) guidance for measuring CYP2C8 inhibition include paclitaxel 6α-hydroxylation (preferred), as well as amodiaquine N-deethylation and rosiglitazone *para*-hydroxylation (acceptable). Repaglinide and rosiglitazone are FDA recommended *in vivo* probe substrates for studying CYP2C8 inhibition (Huang et al., 2007). No studies to our knowledge have compared the inhibition profiles of these probe substrates *in vitro*. Our first aim was to measure the *in vitro* inhibition profiles of three clinically relevant CYP2C8 probe substrates (paclitaxel, repaglinide and rosiglitazone) and amodiaquine (Figure 1) versus a panel of twenty-two known CYP2C8 inhibitors to determine the relative *in vitro* sensitivities of each probe substrate. In addition, the *in vitro* inactivation profiles for each probe substrate versus gemfibrozil 1-O-β-glucuronide, a known mechanism-based inactivator of CYP2C8 (Ogilvie et al., 2006), were determined to evaluate the relative *in vitro* sensitivities towards irreversible inhibition.

DMD Fast Forward. Published on June 22, 2011 as DOI: 10.1124/dmd.111.039065
This article has not been copyedited and formatted. The final version may differ from this version.

Montelukast, a leukotriene-receptor antagonist, is well characterized as a potent and selective inhibitor of CYP2C8 *in vitro* (Walsky et al., 2005). *In vitro* phenotyping studies (Chiba et al., 1997) based on high montelukast concentrations (100-500 μM), indicated that montelukast 21-hydroxylation (M5 formation) is catalyzed by CYP3A and montelukast 36-hydroxylation (M6 formation) by CYP2C9. *In vivo*, montelukast undergoes oxidative metabolism with the majority of the metabolites excreted in bile and less than 1% eliminated in the urine (Balani et al., 1997). After dosing of montelukast, the maximum plasma concentration is usually less than 1 μM (Karonen et al., 2010). The discrepancy in concentrations between the *in vitro* phenotyping experiments and the *in vivo* situation raises the possibility that other P450 isoforms could be involved. In addition, an *in vivo* study using gemfibrozil, whose glucuronide metabolite is a mechanism-based inactivator of CYP2C8, indicated marked inhibition of montelukast *in vivo* and suggested a previously unknown role for CYP2C8 in montelukast metabolism (Karonen et al., 2010). More recent data indicates that CYP2C8 plays a role in the *in vitro* metabolism of montelukast at clinically relevant concentrations (Filppula et al., 2011). Our second aim was to further evaluate the contribution of CYP2C8 in the metabolism of montelukast *in vitro*. Given that montelukast demonstrated CYP2C8 selectivity at clinically relevant concentrations, we also characterized montelukast for its potential as an *in vitro* probe substrate versus the panel of twenty-two known CYP2C8 inhibitors.

The ability to predict changes in the exposure levels of a given drug in the presence of an inhibitor for the *in vivo* situation is useful (Rostami-Hodjegan and Tucker, 2007). The magnitude of a DDI is dependent upon the fraction metabolized (f_m) of a probe substrate for the inhibited pathway. However, no studies to our knowledge have compared the *in vivo* sensitivity of CYP2C8 probe substrates based upon DDI data from the literature, as has been demonstrated for CYP3A4 (Ragueneau-Majlessi et al., 2007;

Foti et al., 2010). Our final aim was to mine the literature for clinical DDI data and to correlate the DDI sensitivity of six probe substrates (cerivastatin, fluvastatin, montelukast, pioglitazone, repaglinide and rosiglitazone) with known contribution to clearance from CYP2C8.

DMD Fast Forward. Published on June 22, 2011 as DOI: 10.1124/dmd.111.039065
This article has not been copyedited and formatted. The final version may differ from this version.

Materials and Methods

Materials. Pooled human liver microsomes (HLMs, 15 individual donors) and individual HLMs were purchased from CellzDirect (Durham, NC) or Xenotech (Lenexa, KS). Recombinant human P450 isoforms (Supersomes™) containing cytochrome b_5 protein (except for CYP1A2 and CYP2D6) and recombinant flavin-containing monooxygenase (FMO) isoforms were purchased from BD Biosciences (Woburn, MA). CYP2C9 monoclonal inhibitory antibody was purchased from Xenotech (Lenexa, KS) and all other P450 selective monoclonal inhibitory antibodies (with ascites fluid) were purchased from BD Biosciences (San Jose, CA). Ammonium formate, HPLC-grade acetonitrile and HPLC-grade methanol were obtained from Alfa Aesar (Ward Hill, MA). NADPH was purchased from EMD Biosciences (San Diego, CA). Montelukast and rosiglitazone were purchased from Cayman Chemical Company (Ann Arbor, MI). Montelukast metabolites (M2, M5 and M6) were purchased from Santa Cruz Biotechnology, Inc (Santa Cruz, CA). The metabolite N-desethylamodiaquine was purchased from BD Biosciences (San Jose, CA). The metabolites N-desmethylrosiglitazone, hydroxypioglitazone and 3'-hydroxyrepaglinide were purchased from Toronto Research Chemicals, Inc (North York, ON, Canada). All other chemicals used were purchased from Sigma-Aldrich (St. Louis, MO) and were of the highest purity available.

K_i Determination. Incubations were carried out using five probe substrates of CYP2C8: amodiaquine, montelukast, paclitaxel, repaglinide and rosiglitazone. Twenty-two known inhibitors of CYP2C8 exhibiting a wide range of inhibition potencies were selected for the *in vitro* studies. Stock solutions of all the inhibitors were made and diluted in acetonitrile:DMSO (90:10) to minimize organic solvent content. Four concentrations of each probe substrate ($0.5xK_m$, K_m, $2xK_m$ and $4xK_m$: K_m = 0.80 μM for amodiaquine; K_m = 0.014 μM for montelukast; K_m = 7.1 μM for paclitaxel; K_m = 3.4 μM for repaglinide; and

K_m= 1.1 μM for rosiglitazone) and five concentrations of each inhibitor (spanning a ten-fold range of the expected K_i) were used for determination of K_i in a 96-well plate format. Briefly, each reaction was carried out in duplicate containing 0.1 mg/mL human liver microsomal protein per incubation. Each incubation reaction mixture contained enzyme, probe substrate and inhibitor suspended in phosphate buffer (100 mM, pH 7.4) containing 3 mM $MgCl_2$ and was preincubated for three minutes in an incubator-shaker at 37 °C. The reactions were initiated by the addition of NADPH (1 mM final concentration). DMSO concentrations did not exceed 0.1% v/v and total organic solvent concentrations did not exceed 0.5% v/v. Solvent concentrations were the same for all experiments and turnover rates did not differ significantly from minimal solvent controls. The reactions were terminated by adding 100 μL of acetonitrile containing 0.1 μM of tolbutamide (internal standard). Lengths of the incubations were 5 minutes, with the exception of paclitaxel, which was run for 10 minutes to increase analytical sensitivity. The incubation time and protein concentrations used were within the linear range for each respective P450 probe reaction. In addition, depletion of the substrate and inhibitor was less than 10% over the reaction time.

K_I and k_{inact} Determination. Time-dependent inactivation experiments were conducted using gemfibrozil 1-O-β-glucuronide as the inactivator and five probe substrates of CYP2C8: amodiaquine, montelukast, paclitaxel, repaglinide and rosiglitazone. Concentrations of gemfibrozil 1-O-β-glucuronide used were 0-50 μM for the primary reactions. Briefly, each primary reaction was carried out in duplicate containing 1.0 mg/mL human liver microsomal protein per incubation. Each primary incubation reaction mixture contained enzyme and inactivator suspended in phosphate buffer (100 mM, pH 7.4) containing 3 mM $MgCl_2$ and was preincubated for three minutes in an incubator-shaker at 37 °C. The reactions were initiated by the addition of NADPH (1 mM final

DMD Fast Forward. Published on June 22, 2011 as DOI: 10.1124/dmd.111.039065
This article has not been copyedited and formatted. The final version may differ from this version.

concentration). At time points of 0, 1, 2, 3, and 5 minutes, 20 µL aliquots were removed and transferred to a secondary incubation (final volume 200 µL) containing probe substrate and 1 mM NADPH in phosphate buffer (100 mM, pH 7.4) containing 3 mM $MgCl_2$. Concentrations of probe substrate used were approximately five-fold above K_m (4 µM for amodiaquine; 0.1 µM for montelukast; 35 µM for paclitaxel; 15 µM for repaglinide and 5 µM for rosiglitazone) for the secondary reaction. The secondary reactions were terminated by adding 100 µL of acetonitrile containing 0.1 µM of tolbutamide (internal standard). Length of the secondary reactions was 5 minutes with the exception of paclitaxel, which was run for 10 minutes to increase analytical sensitivity. The incubation time and protein concentrations used were within the linear range for each respective P450 probe reaction.

Montelukast Kinetics. Michaelis-Menten kinetic parameters K_m and V_{max} were determined over a range of montelukast concentrations (0-0.25 µM) in HLMs and CYP2C8, CYP2C9 and CYP3A4 Supersomes™ for the M2 (sulfoxdation), M5 (21-hydroxylation) and M6 (36-hydroxylation) metabolites. Each incubation reaction mixture contained HLMs (0.1 mg/mL or 0.05 µM of Supersomes™) and montelukast, suspended in phosphate buffer (100 mM, pH 7.4) containing 3 mM $MgCl_2$ and was preincubated for three minutes in an incubator-shaker at 37 °C. The reactions were initiated by the addition of NADPH (1 mM final concentration). The reactions were terminated by adding 100 µL of acetonitrile containing 0.1 µM of ketoconazole (internal standard). Length of the incubations was 5 minutes. Montelukast metabolites were measured by LC/MS/MS as described below.

Montelukast Phenotyping. To determine which P450 isoforms were responsible for montelukast metabolism, we conducted three *in vitro* approaches: (1) immunochemical

DMD Fast Forward. Published on June 22, 2011 as DOI: 10.1124/dmd.111.039065
This article has not been copyedited and formatted. The final version may differ from this version.

inhibition in HLMs; (2) metabolism by P450 supersomes™; and (3) a correlation analysis in HLMs. Immunochemical inhibition studies were performed with anti-human CYP1A2, CYP2B6, CYP2C8, CYP2C9, CYP2C19, CYP2D6, CYP2E1 and CYP3A4 as previously recommended (Gelboin et al., 1995) and per vendor specifications. In brief, 5 µL of pooled human liver microsomes (20 mg/mL) were incubated with 10 µL of the antibody (10 mg/mL) plus 5 µL of TRIS buffer for 30 minutes on ice. The final concentration of antibody was 100 µg/mg of HLMs. The incubation was then diluted to 0.2 mg/mL microsomal protein in 100 mM potassium phosphate buffer (pH 7.4). Ketoconazole (500 nM) was added to the CYP3A4 incubation (Rock et al., 2008). Montelukast was added to the incubation mixture at final concentrations of 0.1 µM. Control P450 substrate marker reactions, as previously reported (Walsky and Obach, 2004), were run to verify the effectiveness of the P450 antibodies. Each incubation reaction mixture contained HLMs, probe substrate or montelukast, suspended in phosphate buffer (100 mM, pH 7.4) containing 3 mM $MgCl_2$ and was preincubated for three minutes in an incubator-shaker at 37 °C. The reactions were initiated by the addition of NADPH (1 mM final concentration). The reactions were terminated by adding 100 µL of acetonitrile containing 0.1 µM of tolbutamide (internal standard). Length of the incubations was 60 minutes. Montelukast metabolites were measured by LC/MS/MS as described below.

P450 Supersomes™ (CYP1A2, CYP2B6, CYP2C8, CYP2C9, CYP2C19, CYP2D6, CYP2E1, CYP3A4 and CYP3A5) at a concentration of 0.05 µM were suspended in phosphate buffer (100 mM, pH 7.4) containing 3 mM $MgCl_2$ and montelukast at a final concentration of 0.1 µM. The incubation mixtures were initiated, quenched and analyzed as described above. Human liver microsomes obtained from 18 individual subjects were incubated with 0.1 µM of montelukast and 0.5 µM midazolam, 40 µM testosterone, 10 µM paclitaxel or 20 µM diclofenac to measure montelukast metabolism and P450 marker activities (Walsky and Obach, 2004). The same reaction

DMD Fast Forward. Published on June 22, 2011 as DOI: 10.1124/dmd.111.039065
This article has not been copyedited and formatted. The final version may differ from this version.

mixtures and incubation conditions as described above were used. The fraction metabolized ($f_{mCYP2C8}$) of montelukast was calculated from the HLM phenotyping experiments by dividing the total amount of M6 formed by the total sum of oxidative metabolism; where the total amount of M6 formation was corrected by the percent contribution of CYP2C8.

Liquid Chromatography/Tandem Mass Spectral Analysis. All analytical methods were conducted using LC-MS/MS technology. For P450 substrate probe reactions, the LC-MS/MS system was comprised of an Applied Biosystems 4000 Q-Trap (operated in triple quadrupole mode) equipped with an electrospray ionization source (Applied Biosystems, Foster City, CA). The MS/MS system was coupled to two LC-20AD pumps with an in-line CBM-20A controller and DGU-$20A_5$ solvent degasser (Shimadzu, Columbia, MD) and a LEAP CTC HTS PAL autosampler equipped with a dual-solvent self-washing system (CTC Analytics, Carrboro, NC). The injection volume was 10 µL for each sample. LC separation was achieved using a Gemini C18 2.0 x 30 mm 5 µm column (Phenomenex, Torrance, CA). Gradient elution (flow rate = 500 µL/minutes) was carried out using a mobile phase system consisting of (A) 5 mM ammonium formate with 0.1% formic acid and (B) acetonitrile with 0.1% formic acid. The solvent flow was diverted from the MS/MS system for the first 20 seconds to remove any non-volatile salts. MS/MS conditions were optimized for individual analytes, accordingly. Generic MS parameters included the curtain gas (10 arbitrary units), CAD gas (medium), ionspray voltage (4500 V), source temperature (450 °C) and ion source gas 1 and gas 2 (40 arbitrary units, each). Interface heaters were kept on for all analytes. Analysis masses were (positive ionization mode): N-desethylamodiaquine, *m/z* 328.1→283.1; N-desmethylrosiglitazone, *m/z* 344.2→121.2; p-3'-hydroxypaclitaxel *m/z* 870.1→105.3; 6α-

hydroxypaclitaxel, *m/z* 870.1→286.2; hydroxypioglitazone, *m/z* 413.1→178.1; 3'-hydroxyrepaglinide, *m/z* 469.1→246.1 and tolbutamide, *m/z* 271.2→91.1. For identification of montelukast metabolites, the LC-MS/MS system was comprised of a TSQ Vantage Triple Stage Quadrupole Mass Spectrometer equipped with a heated electrospray ionization probe (Thermo Electron Corporations, San Jose, CA). The MS/MS system was coupled to an Accela high-speed LC pump and a Thermo Scientific autosampler (Thermo Electron Corporations, San Jose, CA). The injection volume for each sample was 20 µL. LC separation was achieved using a Kinetex C18 2.10 x 50 mm 2.6 µm column (Phenomenex, Torrance, CA). Gradient elution (flow rate = 700 µL/minutes) was carried out using a mobile phase system consisting of (A) 5 mM ammonium formate with 0.1% formic acid plus 1% isopropanol and (B) acetonitrile with 0.1% formic acid. LC flow was diverted from the MS/MS system for the first 2 minutes to remove any non-volatile salts. MS/MS conditions were optimized for individual analytes, accordingly. Generic MS parameters included the curtain gas (10 arbitrary units), CAD gas (high), ion spray voltage (4500 V), source temperature (400 °C) and ion source gas 1 and gas 2 (40 arbitrary units, each). Analysis masses were (positive ionization mode): montelukast, *m/z* 586.2→422.3; M6 (36-hydroxylation), *m/z* 602.2→438.3; M5 (21-hydroxylation), *m/z* 602.2→147.1; M2 (sulfoxidation), *m/z* 602.2→422.3; and ketoconazole, *m/z* 531.2→82.0.

Statistical Analysis. Standard curve fitting was performed using Analyst (version 1.4; Applied Biosystems, Foster City, CA). In general, standard curves were weighted using 1/x. Substrate saturation curves and inhibition data were plotted and analyzed using GraphPad Prism (version 4.01; GraphPad Software Inc., San Diego, CA). Data was

DMD Fast Forward. Published on June 22, 2011 as DOI: 10.1124/dmd.111.039065
This article has not been copyedited and formatted. The final version may differ from this version.

then fit to a competitive (Equation 1), non-competitive (Equation 2), or linear-mixed inhibition model (Equation 3).

(1) $$v = \frac{V_{max} \bullet [S]}{K_m(1+\frac{[I]}{K_i}) + [S]}$$

(2) $$v = \frac{V_{max} \bullet [S]}{K_m(1+\frac{[I]}{K_i}) + [S](1+\frac{[I]}{K_i})}$$

(3) $$v = \frac{V_{max} \bullet [S]}{K_m(1+\frac{[I]}{K_i}) + [S](1+\frac{[I]}{K_i'})}$$

In the preceding equations, K_m is equal to the substrate concentration at half maximal reaction velocity, [I] is the concentration of inhibitor in the system, K_i is the dissociation constant for the enzyme-inhibitor complex and K_i' is the dissociation constant for the enzyme-substrate-inhibitor complex. Note that in the above equations, K_m, K_i, K_i' and V_{max} were treated as global parameters. The mechanism of inhibition was determined by visual inspection of the data using Dixon ([I] vs 1/*v*) and Lineweaver-Burke (1/[S] vs 1/*v*) plots and comparative model assessment using the Akaike Information Criteria. For the inactivation experiments, the natural logarithm decrease in activity over time (k_{obs}) was measured for each inhibitor concentration, which represents the negative slope of the inactivation line. K_I and k_{inact} were determined using the following equation:

(4) $$k_{obs} = k_{obs\ t=0} + \frac{k_{inact} \bullet [I]}{K_I + [I]}$$

In the preceding equation, k_{obs} is equal to the rate of inactivation by the inactivator, $k_{obs\ t=0}$ is equal to the rate of inactivation by the inactivator at time = 0, k_{inact} is the maximal rate

of inactivation, K_I is equal to the inactivator concentration at half maximal rate of inactivation and [I] is the concentration of inactivator.

*Correlation Analysis of In Vivo Drug Interaction Potential***.** Literature data for AUC_I/AUC were obtained using the University of Washington Metabolism and Transport Drug Interaction Database™, where AUC_I is defined as the area under the plasma concentration-time curve for a given probe substrate in the presence of an inhibitor and AUC is defined as the area under the plasma concentration-time curve for a given probe substrate in the absence of inhibitor. Studies were considered comparable if they had a similar dose regimen for both inhibitor and probe substrate. For instances where multiple AUC_I/AUC values were available in the literature, the AUC_I/AUC values were averaged.

Prediction of In Vivo Drug Interactions.

Prediction of inactivation DDIs were made using Equation 5 (Mayhew, 2000):

(5) $$\partial AUC = \frac{AUC_I}{AUC} = \frac{1}{\frac{f_{mCYP}}{1+(\frac{k_{inact}[I]_{h,u}}{K_I * k_{deg}})} + (1 - f_{mcyp})}$$

Where f_{mCYP} is the fraction of probe substrate cleared by the indicated P450, $[I]_{h,u}$ is the maximum unbound hepatic input concentration, k_{inact} is the maximal rate of inactivation, K_I is the concentration of inactivator at half maximal rate of inactivation and k_{deg} is the degradation rate of CYP2C8 [0.0005 days, (Lai et al., 2009)]. For the predictions using gemfibrozil-1-*O*-β-glucoronide as inhibitor, the following inputs were used: $f_{mCYP2C8}$ values of 0.81, 0.63, 0.49 and 0.50 for montelukast, pioglitazone, repaglinide and rosiglitazone, respectively (Hinton et al., 2008)

Results

The inhibition constants (K_i) for a set of twenty-two effectors were determined for the probe substrates amodiaquine, montelukast, paclitaxel, repaglinide and rosiglitazone *in vitro* (Table 1, structures in Figure 1). Competitive inhibition profiles were observed in all cases. Repaglinide was the most sensitive probe substrate, followed by amodiaquine, rosiglitazone, and montelukast, while paclitaxel exhibited marked differences in observed inhibition potency from the other probe substrates. In addition to the set of competitive inhibition constants (K_i), inactivation kinetic constants (K_I and k_{inact}) for gemfibrozil-1-*O*-β-glucoronide, a mechanism-based inhibitor of CYP2C8, were determined for the five probe substrates. There was a range of values observed among the five probe substrates, with the K_I ranging from 10 to 49 μM and the k_{inact} ranging from 0.02 to 0.08 minutes^{-1} (Table 2). The magnitude of *in vivo* DDI caused by gemfibrozil-1-*O*-β-glucoronide was predicted for the clinically relevant probe substrates pioglitazone, repaglinide, rosiglitazone and montelukast (Table 2).

In pooled human liver microsomes, the oxidation of montelukast resulted in the formation of three major metabolites (M2, M5 and M6; Figure 2). Michaelis-Menten kinetic parameters (K_m and V_{max}) were determined for the oxidative metabolism of montelukast over a concentration range of 0-0.25 μM in HLMs and CYP2C8, CYP3A4 and CYP2C9 Supersomes™ (Figure 3). Over the range of concentrations formation of M6 (36-hydroxylation) was linear in both CYP2C9 and CYP3A4 Supersomes™. In CYP2C8 Supersomes™ and HLMs the formation of M6 (36-hydroxylation) followed Michael-Menten kinetics and the K_m was determined to be 14 nM and 65 nM, respectively. A panel of nine P450 enzymes (Supersomes™) was incubated with montelukast (Figure 4A-4C). The formation of M2 (sulfoxidation) and M5 (21-hydroxylation) were inhibited with the CYP3A inhibitor ketoconazole (500 nM) plus a CYP3A selective antibody, a combination known to produce a more complete and

selective inhibition than either alone ((Rock et al., 2008), Figure 4E and 4F)). Formation of M6 (36-hydroxylation) was inhibited by a selective CYP2C8 antibody (Figure 4D). Both results revealed similar profiles, with CYP3A4 and CYP2C8 as the major P450 enzymes involved in the turnover of montelukast. Montelukast did not appear to be metabolized by flavin-containing monooxygenase (FMO), in agreement with previous results (Chiba et al., 1997). In addition, correlation analysis across a bank of 18 individual human liver microsomes showed a significant correlation coefficient between the CYP2C8-selective formation of 6α-hydroxypaclitaxel and the M6 (36-hydroxylation) oxidative metabolite of montelukast (0.1 μM) with an r^2=0.89 (Figure 5). The CYP3A metabolism of 1'-hydroxymidazolam and 6-*β* hydroxytestosterone also demonstrated a correlation coefficient with the M2 (sulfoxdation) and M5 (21-hydroxylation) oxidative metabolite of montelukast with r^2 values greater than 0.84 (data not shown).

The metabolism of cerivastatin, fluvastatin, montelukast, pioglitazone, repaglinide and rosiglitazone is partially mediated by CYP2C8 *in vivo*. *In vivo* DDI results for those compounds were collected from the literature and compiled (Table 3). A linear correlation analysis was carried out on the non-transformed data relative to repaglinide; the CYP2C8 probe substrate with the largest number of comparative DDI studies. All probe substrates exhibited lower sensitivity relative to repaglinide. Of currently prescribed probe substrates, the rank in order of decreasing sensitivity was montelukast, pioglitazone, rosiglitazone and fluvastatin.

Discussion

Drug-drug interactions are one of the primary causes of serious adverse events occurring in clinical practice (Huang et al., 2007). A crucial part of the drug discovery and development paradigm is screening for and predicting the magnitude of P450-mediated DDIs. Examples of drugs withdrawn from the market due to drug interactions include mibefradil (Po and Zhang, 1998) and cerivastatin (Davidson, 2002). Cerivastatin was withdrawn from the market after 500 adverse events; almost half of the events were directly correlated with co-administration of the CYP2C8 inhibitor gemfibrozil (Farmer, 2001; Backman et al., 2002).

In vitro inhibition studies serve as a basis for *in vivo* DDI predictions. Probe substrate-dependent inhibition has been demonstrated for CYP2C9 (Kumar et al., 2006), CYP2C19 (Foti and Wahlstrom, 2008) and CYP3A4 (Kenworthy et al., 1999; Stresser et al., 2000; Foti et al., 2010) and may confound predictions of the *in vivo* situation. Selection of a probe substrate that is applicable to both the *in vitro* and *in vivo* situations may reduce the impact of probe substrate-dependent inhibition on prediction accuracy. Therefore, a comprehensive understanding of *in vitro* and *in vivo* applicability and sensitivity enables appropriate probe substrate selection.

Our selection of *in vitro* probe substrates was based upon recommendations from the FDA guidance and the availability of clinical DDI data. Amodiaquine, paclitaxel and rosiglitazone have been used as CYP2C8 *in vitro* probe substrates (Walsky et al., 2005). Repaglinide was selected due to the availability of clinical DDI results (Huang et al., 2007), whereas montelukast was selected based on a recent report of CYP2C8-mediated metabolism *in vivo* (Karonen et al., 2010). Repaglinide exhibited the greatest sensitivity as an *in vitro* probe. Relative to repaglinide, a 3-fold average decrease in inhibition potency was observed for rosiglitazone and amodiaquine and a 4-fold decrease for montelukast. Paclitaxel displayed a 15-fold average decrease in observed

inhibition potency relative to repaglinide. Based upon these results, CYP2C8 exhibited probe substrate-dependent inhibition.

Plausible mechanisms for probe substrate-dependent inhibition observed *in vitro* include the presence of multiple binding regions within the P450 active site, metabolic switching and the involvement of more than one enzyme in metabolite formation (Kenworthy et al., 1999; Regal et al., 2005). The elucidation of the crystal structure of CYP2C8 has provided useful information on how ligands interact with this enzyme and how CYP2C members determine probe substrate specificity. In the ligand-free structure of CYP2C8, the large active site cavity exhibits architecture that approximates a T or Y shape with branches of differing lengths, widths and chemical properties (Schoch et al., 2004; Schoch et al., 2008). The crystal structures of CYP2C8 with felodipine, montelukast or troglitazone bound demonstrate distinct binding interactions to the CYP2C8 active site: montelukast fills the entire structure of CYP2C8, felodipine occupies the active site cavity near the heme and troglitazone fills the upper portion of the active site, indicating that the probe substrates occupy distinct, although potentially overlapping, binding regions within the active site (Schoch et al., 2008). Paclitaxel produces two metabolites, 6α-hydroxylpaclitaxel (CYP2C8) and *p*-3'-hydroxypaclitaxel (CYP3A4), such that metabolic switching is another plausible explanation for the distinctive decrease in sensitivity to inhibition. However, formation of *p*-3'-hydroxypaclitaxel did not increase upon addition of the inhibitors, indicating that metabolic switching did not occur (data not shown). Additionally, the formation of 6α-hydroxylpaclitaxel was demonstrated to be selective for CYP2C8 (Rahman et al., 1994). When taken together, the CYP2C8 results suggest that specific probe substrate-P450 active site interactions may have a marked affect on enzyme inhibition and distinguish between probe substrates that share some overlap in binding modes.

The probe substrate montelukast is a leukotriene-receptor antagonist and a known inhibitor of CYP2C8. Although montelukast is a potent and selective inhibitor of CYP2C8 *in vitro* (Walsky et al., 2005), it does not alter the clearance of pioglitazone or repaglinide *in vivo* (Jaakkola et al., 2006; Kajosaari et al., 2006). More recently, gemfibrozil was shown to markedly increase the plasma concentrations of montelukast, implying that CYP2C8 may contribute to the elimination of montelukast (Karonen et al., 2010). Experiments were carried out to further evaluate which P450 enzymes were responsible the *in vitro* metabolism of montelukast. Three P450-mediated metabolites of montelukast are M2 (sulfoxdation), M5 (21-hydroxylation) and M6 (36-hydroxylation) as shown in Figure 2 (Chiba et al., 1997).

According to prescribing information and *in vitro* studies, CYP3A4 and CYP2C9 are the main P450 enzymes involved in the formation of M2 (sulfoxdation)/M5 (21-hydroxylation) and M6 (36-hydroxylation), respectively. However, at the time of the montelukast phenotyping experiments the *in vitro* tools to evaluate CYP2C8 were lacking. More so, the high montelukast concentrations (100-500 μM) used in the experiments (100 to 1,000-fold higher than therapeutic total plasma concentrations) would have saturated the CYP2C8-mediated metabolism and confounded the results. More recently, *in vivo* administration of gemfibrozil greatly impaired the elimination of M6 (Karonen et al., 2010). In addition, CYP2C8 has been shown to be crucial in the *in vitro* metabolism of montelukast at clinically relevant concentrations (Filppula et al., 2011). Here, additional *in vitro* experiments were performed, including correlation analysis, phenotyping experiments with selective antibodies and *in vitro* kinetics to further characterize the *in vitro* metabolism of montelukast by CYP2C8. Montelukast concentrations in plasma range between 0.05 and 0.80 μM (Karonen et al., 2010); therefore, in order to approximate these conditions, low montelukast concentrations were used in our microsomal incubation. At low montelukast concentrations (0-0.25

DMD Fast Forward. Published on June 22, 2011 as DOI: 10.1124/dmd.111.039065
This article has not been copyedited and formatted. The final version may differ from this version.

μM), the formation of M6 was predominantly mediated by CYP2C8, not CYP2C9 or CYP3A4 (Figure 4). In contrast, administration of gemfibrozil did not reduce the formation of M5 (21-hydroxylation), in agreement that CYP3A4 is responsible for its formation (Chiba et al., 1997). Together, these results indicate that at clinically relevant concentrations, metabolism by CYP2C8 is a major determinant in the elimination of montelukast.

The mechanism of CYP2C8 inactivation by gemfibrozil-1-*O*-β-glucoronide is the formation of a benzyl radical intermediate that binds to the γ-meso position of the prosthetic heme and renders CYP2C8 catalytically inactive (Baer et al., 2007). The inactivation kinetic parameters (K_I and k_{inact}) across five probe substrates (Table 2) were determined. As expected for mechanisms that inactivate through heme modification, the kinetic inactivation parameters between probe substrates were similar. These differences observed also did not play a role in changing the *in vivo* predictions, as a key characteristic impacting DDI predictions is the fraction metabolized by the specific P450 (f_{mCYP}) enzyme. Predictions for inhibition by gemfibrozil-1-*O*-β-glucoronide were driven by the $f_{mCYP2C8}$ (Hinton et al., 2008) and were insensitive to substrates with $f_{mCYP2C8}$ values less than 0.65. Using our *in vitro* kinetic parameters for inactivation by gemfibrozil-1-*O*-β-glucoronide (Table 2) and the $f_{mCYP2C8}$ of montelukast (0.81), our prediction AUC_I/AUC was within 10% of the observed value. Collectively, the P450-phenotyping and DDI predictions indicate that CYP2C8 is the primary enzyme involved in the oxidation of montelukast at clinically relevant substrate concentrations.

The *in vivo* sensitivity of the CYP2C8 probe substrates may influence selection of CYP2C8 probe substrate for a clinical study. Retrospective analysis of clinical DDI studies from the literature has been used to correlate the relative sensitivity of probe substrates *in vivo* based upon results from multiple CYP3A4 inhibitors (Ragueneau-Majlessi et al., 2007; Foti et al., 2010). The availability of clinical DDI studies relative to

DMD Fast Forward. Published on June 22, 2011 as DOI: 10.1124/dmd.111.039065
This article has not been copyedited and formatted. The final version may differ from this version.

repaglinide and a known contribution of CYP2C8 to clearance were our selection criteria for inclusion in the *in vivo* correlation analysis. The DDI results were averaged for instances where multiple clinical studies for the same inhibitor and probe substrate combination were available and carried out using similar conditions. All of the probe substrates displayed reduced sensitivity relative to repaglinide. Although cerivastatin and repaglinide were sensitive to inhibition by gemfibrozil *in vivo*, both are substrates of OATP1B1; observed DDI *in vivo* may be due to a combination of metabolism and transporter inhibition (Hinton et al., 2008). Gemfibrozil-1-*O*-β-glucoronide, a key component for the *in vivo* sensitivity analysis presented here, is an inhibitor of both CYP2C8 and OATP1B1 (Shitara et al., 2004). Therefore, consideration of confounding factors such as transporter-mediated clearance may aid in selecting an appropriate probe substrate for a clinical DDI study.

The selection of a CYP2C8 probe substrate for *in vitro* experiments and clinical DDI studies impacts both the measured inhibition potency *in vitro* and the observed magnitude of DDI *in vivo*. The results presented here indicate that probe selection for CYP2C8 is important. Amodiaquine is a sensitive CYP2C8 *in vitro* probe substrate but lacks marketing approval in the United States; testing an unusual *in vitro* result with amodiaquine in the clinic would therefore be difficult. Paclitaxel was the least sensitive *in vitro* probe substrate, exhibits a narrow therapeutic index and has pharmacokinetics *in vivo* that are substantially altered by inhibitors of P-glycoprotein; therefore, it is an unfavorable CYP2C8 probe substrate for both the *in vitro* and *in vivo* situations. The use of repaglinide as a probe substrate is limited because of confounding issues with transporter interactions (OATP1B1) and the potential for hypoglycemia (Roustit et al., 2010). Rosiglitazone (and pioglitazone) have acceptable *in vitro* and *in vivo* characteristics, moderate $f_{mCYP2C8}$ values and may be appropriate CYP2C8 probe substrates depending upon the therapeutic area of the new chemical entity and the

DMD Fast Forward. Published on June 22, 2011 as DOI: 10.1124/dmd.111.039065
This article has not been copyedited and formatted. The final version may differ from this version.

drugs that are likely to be co-administered. Based upon its *in vitro* and *in vivo* sensitivity, safety profile and high $f_{mCYP2C8}$ value (0.81), montelukast is an appropriate choice for CYP2C8 probe substrate. Overall, due to the demonstrated potential for probe substrate-dependent inhibition *in vitro* and *in vivo*, careful considerations should be taken when selecting a probe substrate for *in vitro* studies. When practical, we recommend that the probe substrate used for *in vitro* studies also be used for the clinical DDI study.

Author Contribution

Participated in research design: VandenBrink, BM; Foti, RS; Rock, DA; Wienkers, LC; Wahlstrom, JL

Conducted experiments: VandenBrink, BM

Contributed new reagents or analytic tools: none

Performed data analysis: VandenBrink, BM; Foti, RS; Wahlstrom, JL

Wrote or contributed to the writing of the manuscript: VandenBrink, BM; Foti, RS; Rock, DA; Wienkers, LC; Wahlstrom, JL

References

Backman JT, Kyrklund C, Neuvonen M, and Neuvonen PJ (2002) Gemfibrozil greatly increases plasma concentrations of cerivastatin. *Clin Pharmacol Ther* **72:**685-691.

Baer BR, Wienkers LC, and Rock DA (2007) Time-dependent inactivation of P450 3A4 by raloxifene: identification of Cys239 as the site of apoprotein alkylation. *Chem Res Toxicol* **20:**954-964.

Balani SK, Xu X, Pratha V, Koss MA, Amin RD, Dufresne C, Miller RR, Arison BH, Doss GA, Chiba M, Freeman A, Holland SD, Schwartz JI, Lasseter KC, Gertz BJ, Isenberg JI, Rogers JD, Lin JH, and Baillie TA (1997) Metabolic profiles of montelukast sodium (Singulair), a potent cysteinyl leukotriene1 receptor antagonist, in human plasma and bile. *Drug Metab Dispos* **25:**1282-1287.

Chiba M, Xu X, Nishime JA, Balani SK, and Lin JH (1997) Hepatic microsomal metabolism of montelukast, a potent leukotriene D4 receptor antagonist, in humans. *Drug Metab Dispos* **25:**1022-1031.

Davidson MH (2002) Controversy surrounding the safety of cerivastatin. *Expert opinion on drug safety* **1:**207-212.

Deng LJ, Wang F, and Li HD (2005) Effect of gemfibrozil on the pharmacokinetics of pioglitazone. *Eur J Clin Pharmacol* **61:**831-836.

Farmer JA (2001) Learning from the cerivastatin experience. *Lancet* **358:**1383-1385.

Filppula AM, Laitila J, Neuvonen PJ, and Backman JT (2011) Reevaluation of the Microsomal Metabolism of Montelukast - Major Contribution by CYP2C8 at Clinically Relevant Concentrations *Drug Metab Dispos, ePub ahead of print*.

Foti RS, Rock DA, Wienkers LC, and Wahlstrom JL (2010) Selection of Alternative CYP3A4 Probe Substrates for Clinical Drug Interaction Studies Using In Vitro Data and In Vivo Simulation. *Drug Metab Dispos* **38:**981-987.

Foti RS and Wahlstrom JL (2008) CYP2C19 inhibition: the impact of substrate probe selection on in vitro inhibition profiles. *Drug metabolism and disposition: the biological fate of chemicals* **36:**523-528.

Gelboin HV, Krausz KW, Goldfarb I, Buters JT, Yang SK, Gonzalez FJ, Korzekwa KR, and Shou M (1995) Inhibitory and non-inhibitory monoclonal antibodies to human cytochrome P450 3A3/4. *Biochem Pharmacol* **50:**1841-1850.

Hatorp V and Thomsen MS (2000) Drug interaction studies with repaglinide: repaglinide on digoxin or theophylline pharmacokinetics and cimetidine on repaglinide pharmacokinetics. *J Clin Pharmacol* **40:**184-192.

Hinton LK, Galetin A, and Houston JB (2008) Multiple inhibition mechanisms and prediction of drug-drug interactions: status of metabolism and transporter models as exemplified by gemfibrozil-drug interactions. *Pharm Res* **25:**1063-1074.

Hruska MW, Amico JA, Langaee TY, Ferrell RE, Fitzgerald SM, and Frye RF (2005) The effect of trimethoprim on CYP2C8 mediated rosiglitazone metabolism in human liver microsomes and healthy subjects. *Br J Clin Pharmacol* **59:**70-79.

Huang SM, Temple R, Throckmorton DC, and Lesko LJ (2007) Drug interaction studies: study design, data analysis, and implications for dosing and labeling. *Clin Pharmacol Ther* **81:**298-304.

Jaakkola T, Backman JT, Neuvonen M, and Neuvonen PJ (2005) Effects of gemfibrozil, itraconazole, and their combination on the pharmacokinetics of pioglitazone. *Clin Pharmacol Ther* **77:**404-414.

Jaakkola T, Backman JT, Neuvonen M, Niemi M, and Neuvonen PJ (2006) Montelukast and zafirlukast do not affect the pharmacokinetics of the CYP2C8 substrate pioglitazone. *Eur J Clin Pharmacol* **62:**503-509.

Kajosaari LI, Niemi M, Backman JT, and Neuvonen PJ (2006) Telithromycin, but not montelukast, increases the plasma concentrations and effects of the cytochrome P450 3A4 and 2C8 substrate repaglinide. *Clin Pharmacol Ther* **79:**231-242.

Karonen T, Filppula A, Laitila J, Niemi M, Neuvonen PJ, and Backman JT (2010) Gemfibrozil markedly increases the plasma concentrations of montelukast: a previously unrecognized role for CYP2C8 in the metabolism of montelukast. *Clin Pharmacol Ther* **88:**223-230.

Kenworthy KE, Bloomer JC, Clarke SE, and Houston JB (1999) CYP3A4 drug interactions: correlation of 10 in vitro probe substrates. *British journal of clinical pharmacology* **48:**716-727.

Kim KA, Park PW, Kim KR, and Park JY (2007) Effect of multiple doses of montelukast on the pharmacokinetics of rosiglitazone, a CYP2C8 substrate, in humans. *Br J Clin Pharmacol* **63:**339-345.

Kivisto KT, Kantola T, and Neuvonen PJ (1998) Different effects of itraconazole on the pharmacokinetics of fluvastatin and lovastatin. *Br J Clin Pharmacol* **46:**49-53.

Kumar V, Wahlstrom JL, Rock DA, Warren CJ, Gorman LA, and Tracy TS (2006) CYP2C9 inhibition: impact of probe selection and pharmacogenetics on in vitro inhibition profiles. *Drug metabolism and disposition: the biological fate of chemicals* **34:**1966-1975.

Lai XS, Yang LP, Li XT, Liu JP, Zhou ZW, and Zhou SF (2009) Human CYP2C8: structure, substrate specificity, inhibitor selectivity, inducers and polymorphisms. *Curr Drug Metab* **10:**1009-1047.

Mayhew BS, Jones, D. R., Hall, S. D. (2000) An In Vitro Model for Predicting In Vivo Inhibition of Cytochrome P450 3A4 by Metabolic Intermediate Complex Formation. *Drug Metabolism and Disposition* **28:**1031-1037.

Mazzu AL, Lasseter KC, Shamblen EC, Agarwal V, Lettieri J, and Sundaresen P (2000) Itraconazole alters the pharmacokinetics of atorvastatin to a greater extent than either cerivastatin or pravastatin. *Clin Pharmacol Ther* **68:**391-400.

Melet A, Marques-Soares C, Schoch GA, Macherey AC, Jaouen M, Dansette PM, Sari MA, Johnson EF, and Mansuy D (2004) Analysis of human cytochrome P450 2C8 substrate specificity using a substrate pharmacophore and site-directed mutants. *Biochemistry* **43:**15379-15392.

Muck W, Ritter W, Dietrich H, Frey R, and Kuhlmann J (1997) Influence of the antacid Maalox and the H2-antagonist cimetidine on the pharmacokinetics of cerivastatin. *Int J Clin Pharmacol Ther* **35:**261-264.

Niemi M, Backman JT, Granfors M, Laitila J, Neuvonen M, and Neuvonen PJ (2003a) Gemfibrozil considerably increases the plasma concentrations of rosiglitazone. *Diabetologia* **46:**1319-1323.

Niemi M, Backman JT, Neuvonen M, and Neuvonen PJ (2003b) Effects of gemfibrozil, itraconazole, and their combination on the pharmacokinetics and pharmacodynamics of repaglinide: potentially hazardous interaction between gemfibrozil and repaglinide. *Diabetologia* **46:**347-351.

Niemi M, Backman JT, and Neuvonen PJ (2004a) Effects of trimethoprim and rifampin on the pharmacokinetics of the cytochrome P450 2C8 substrate rosiglitazone. *Clin Pharmacol Ther* **76:**239-249.

Niemi M, Kajosaari LI, Neuvonen M, Backman JT, and Neuvonen PJ (2004b) The CYP2C8 inhibitor trimethoprim increases the plasma concentrations of repaglinide in healthy subjects. *Br J Clin Pharmacol* **57:**441-447.

Ogilvie BW, Zhang D, Li W, Rodrigues AD, Gipson AE, Holsapple J, Toren P, and Parkinson A (2006) Glucuronidation converts gemfibrozil to a potent,

metabolism-dependent inhibitor of CYP2C8: implications for drug-drug interactions. *Drug Metab Dispos* **34:**191-197.

Po AL and Zhang WY (1998) What lessons can be learnt from withdrawal of mibefradil from the market? *Lancet* **351:**1829-1830.

Ragueneau-Majlessi I, Boulenc X, Rauch C, Hachad H, and Levy RH (2007) Quantitative correlations among CYP3A sensitive substrates and inhibitors: literature analysis. *Curr Drug Metab* **8:**810-814.

Rahman A, Korzekwa KR, Grogan J, Gonzalez FJ, and Harris JW (1994) Selective biotransformation of taxol to 6 alpha-hydroxytaxol by human cytochrome P450 2C8. *Cancer Res* **54:**5543-5546.

Regal KA, Kunze KL, Peter RM, and Nelson SD (2005) Oxidation of caffeine by CYP1A2: isotope effects and metabolic switching. *Drug Metab Dispos* **33:**1837-1844.

Rock DA, Foti RS, and Pearson JT (2008) The combination of chemical and antibody inhibitors for superior P450 3A inhibition in reaction phenotyping studies. *Drug Metab Dispos* **36:**2410-2413.

Rostami-Hodjegan A and Tucker GT (2007) Simulation and prediction of in vivo drug metabolism in human populations from in vitro data. *Nature reviews* **6:**140-148.

Roustit M, Blondel E, Villier C, Fonrose X, and Mallaret MP (2010) Symptomatic hypoglycemia associated with trimethoprim/sulfamethoxazole and repaglinide in a diabetic patient. *Ann Pharmacother* **44:**764-767.

Schoch GA, Yano JK, Sansen S, Dansette PM, Stout CD, and Johnson EF (2008) Determinants of cytochrome P450 2C8 substrate binding: structures of complexes with montelukast, troglitazone, felodipine, and 9-cis-retinoic acid. *J Biol Chem* **283:**17227-17237.

Schoch GA, Yano JK, Wester MR, Griffin KJ, Stout CD, and Johnson EF (2004) Structure of human microsomal cytochrome P450 2C8. Evidence for a peripheral fatty acid binding site. *J Biol Chem* **279:**9497-9503.

Shitara Y, Hirano M, Sato H, and Sugiyama Y (2004) Gemfibrozil and its glucuronide inhibit the organic anion transporting polypeptide 2 (OATP2/OATP1B1:SLC21A6)-mediated hepatic uptake and CYP2C8-mediated metabolism of cerivastatin: analysis of the mechanism of the clinically relevant drug-drug interaction between cerivastatin and gemfibrozil. *J Pharmacol Exp Ther* **311:**228-236.

Spence JD, Munoz CE, Hendricks L, Latchinian L, and Khouri HE (1995) Pharmacokinetics of the combination of fluvastatin and gemfibrozil. *Am J Cardiol* **76:**80A-83A.

Stresser DM, Blanchard AP, Turner SD, Erve JC, Dandeneau AA, Miller VP, and Crespi CL (2000) Substrate-dependent modulation of CYP3A4 catalytic activity: analysis of 27 test compounds with four fluorometric substrates. *Drug metabolism and disposition: the biological fate of chemicals* **28:**1440-1448.

Tornio A, Niemi M, Neuvonen M, Laitila J, Kalliokoski A, Neuvonen PJ, and Backman JT (2008a) The effect of gemfibrozil on repaglinide pharmacokinetics persists for at least 12 h after the dose: evidence for mechanism-based inhibition of CYP2C8 in vivo. *Clin Pharmacol Ther* **84:**403-411.

Tornio A, Niemi M, Neuvonen PJ, and Backman JT (2008b) Trimethoprim and the CYP2C8*3 allele have opposite effects on the pharmacokinetics of pioglitazone. *Drug Metab Dispos* **36:**73-80.

Wahlstrom JL, Rock DA, Slatter GS, and Wienkers LC (2006) Advances in Predicting CYP-Mediated Drug Interactions in the Drug Discovery Setting. *Expert Opin Drug Discov* **1:**677-691.

Walsky RL, Gaman EA, and Obach RS (2005) Examination of 209 drugs for inhibition of cytochrome P450 2C8. *J Clin Pharmacol* **45:**68-78.

Walsky RL and Obach RS (2004) Validated assays for human cytochrome P450 activities. *Drug Metab Dispos* **32:**647-660.

Wienkers LC and Heath TG (2005) Predicting in vivo drug interactions from in vitro drug discovery data. *Nature reviews* **4:**825-833.

Figure Legends

Figure 1. CYP2C8 probe substrate structures: A) amodiaquine, B) paclitaxel, C) repaglinide and D) rosiglitazone. The arrows indicate site of metabolism by CYP2C8 used to determine inhibition constants (K_i).

Figure 2. The chemical structures of montelukast and the major P450-mediated metabolites M2 (sulfoxdation), M5 (21-hydroxylation) and M6 (36-hydroxylation).

Figure 3. The rate of 36-hydroxylation (M6) versus montelukast concentration in (A) CYP2C8 Supersomes™ and (B) human liver microsomes.

Figure 4. (A-C) Cytochrome P450 metabolism of montelukast (0.01 μM) to M6 (36-hydroxylation), M2 (sulfoxdation) and M5 (21-hydroxylation), respectively. (D-F) Percent inhibition by P450 selective monoclonal antibodies of montelukast metabolites M6 (36-hydroxylation), M2 (sulfoxdation) and M5 (21-hydroxylation), respectively.

Figure 5. Cytochrome P450 isoform selective markers (A) CYP2C8, (B) CYP2C9 and (C) CYP3A4 correlated to the formation of montelukast metabolite (M6) in 18 human liver microsomal preparations. The area ratio is equal to the area of the analyte divided by the area of the internal standard.

DMD Fast Forward. Published on June 22, 2011 as DOI: 10.1124/dmd.111.039065
This article has not been copyedited and formatted. The final version may differ from this version.

Table 1. K_i values (μM) obtained using pooled HLMs[a]

	Probe Substrate[b]				
Effector	AMO	MTK	PAC	REP	ROS
Amodiaquine	x[c]	11.7	>100	1.9	11.0
Benzbromarone	0.055	0.38	0.95	0.15	0.36
Celebrex	4.9	7.9	54.4	3.1	5.1
Cerivastatin	4.2	4.6	77.4	4.4	13.4
Clotrimazole	0.12	0.27	0.22	0.19	1.9
Estradiol	6.6	23.8	17.7	8.9	23.8
Gemfibrozil	10.2	13.5	>100	9.3	36.1
Gemfibrozil glucoronide	6.2	4.1	>100	0.99	5.1
Lovastatin	5.6	9.3	18.8	2.8	4.2
Medroxyprogesterone	0.76	7.5	8.2	1.9	6.6
Montelukast	0.0081	x	0.026	0.016	0.21
Nifedipine	2.4	6.3	9.5	1.5	5.8
Paclitaxel	5.4	89.8	x	6.5	12.0
Pioglitzone	6.6	7.1	37.6	3.8	6.1
Quercetin	0.49	0.52	3.0	0.61	0.61
Repaglinide	27.1	11.1	>100	x	23.0
Rosiglitazone	5.2	4.1	28.6	1.4	x
Sertraline	>100	9.0	>100	7.8	8.1
Simvastatin	7.5	5.7	12.3	1.1	3.3
Tamoxifen	3.1	2.1	12.2	10.1	2.6
Triaminocolone	32.5	53.1	>100	42.5	20.4
Trimethoprim	9.2	>100	>100	8.5	13.2

[a] Global standard error for data fitting was less than 20% and $r^2 > 0.90$ for each effector

[b] Abbreviations: Amodiaquine (AMO); Montelukast (MTK); Paclitaxel (PAC); Repaglinide (REP); and Rosiglitazone (ROS)

[c] X denotes an undetermined value

DMD Fast Forward. Published on June 22, 2011 as DOI: 10.1124/dmd.111.039065
This article has not been copyedited and formatted. The final version may differ from this version.

Table 2. Inactivation parameters for gemfibrozil 1-O-β-glucuronide obtained using pooled HLMs[a]

	Probe Substrate[b]					
	AMO	PAC	REP	ROS	MTK	PIO
K_I	10.1	35	18.4	48.5	21.3	33.6
k_{inact}	0.041	0.022	0.035	0.071	0.050	0.082
Predicted AUC_I/AUC	NA[c]	NA	1.9	2.0	5.2	2.6

[a] K_I and k_{inact} are defined by Eq. 4, AUC_I/AUC predictions are defined by Eq.5

[b] Abbreviations: Amodiaquine (AMO); Paclitaxel (PAC); Repaglinide (REP); Rosiglitazone (ROS); Montelukast (MTK); and Pioglitazone (PIO)

[c] Predictions were not made due to unknown $f_{mCYP2C8}$ *in vivo*

DMD Fast Forward. Published on June 22, 2011 as DOI: 10.1124/dmd.111.039065
This article has not been copyedited and formatted. The final version may differ from this version.

Table 3. AUC_I/AUC values obtained from the literature

	AUC_I/AUC[a]						
Inhibitor (mg/day)	CER	FLV	MTK	PIO	REP	ROS	references
Cimetidine (1000-1200 mg)	1.0				1.2		[c]
Gemfibrozil (1200 mg)[b]	5.6	1.1	4.5	3.3	7.7	2.3	[d]
Itraconazole (100-200 mg)	1.3	0.9		1.1	1.4		[e]
Montelukast (10 mg)				1.0	1.0	1.0	[f]
Telithromycin (800 mg)			1.0		1.8		[g]
Trimethoprim (320-400 mg)				1.4	1.6	1.4	[h]

[a]Abbreviations: Cerivastatin (CER); Fluvastatin (FLV); Montelukast (MTK); Pioglitazone (PIO); Repaglinide (REP); Rosiglitazone (ROS)
[b] Gemfibrozil glucuronide is a time-dependent inactivator of CYP2C8
[c] (Muck et al., 1997; Hatorp and Thomsen, 2000)
[d] (Spence et al., 1995; Backman et al., 2002; Niemi et al., 2003a; Niemi et al., 2003b; Niemi et al., 2004a; Deng et al., 2005; Jaakkola et al., 2005; Tornio et al., 2008a; Karonen et al., 2010)
[e] (Kivisto et al., 1998; Mazzu et al., 2000; Niemi et al., 2003b; Jaakkola et al., 2005)
[f] (Jaakkola et al., 2006; Kajosaari et al., 2006; Kim et al., 2007)
[g] (Kajosaari et al., 2006)
[h] (Niemi et al., 2004a; Niemi et al., 2004b; Hruska et al., 2005; Tornio et al., 2008b)

Figure 1

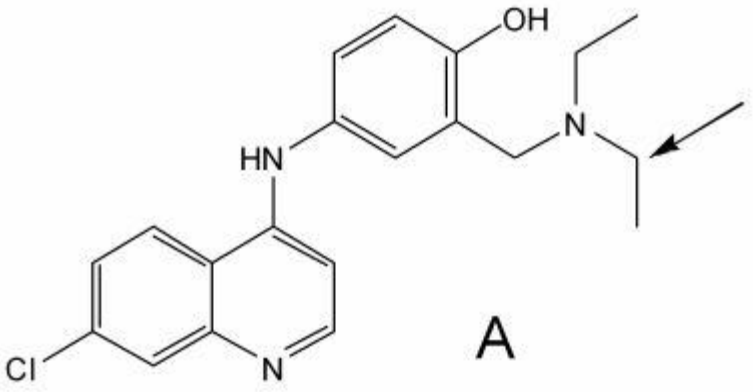

A

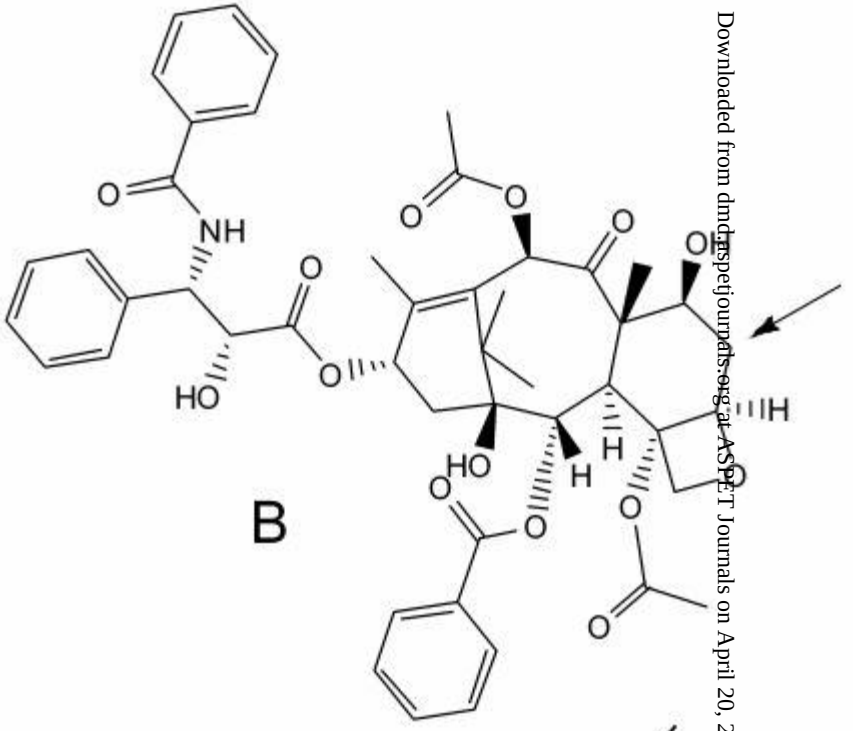

B

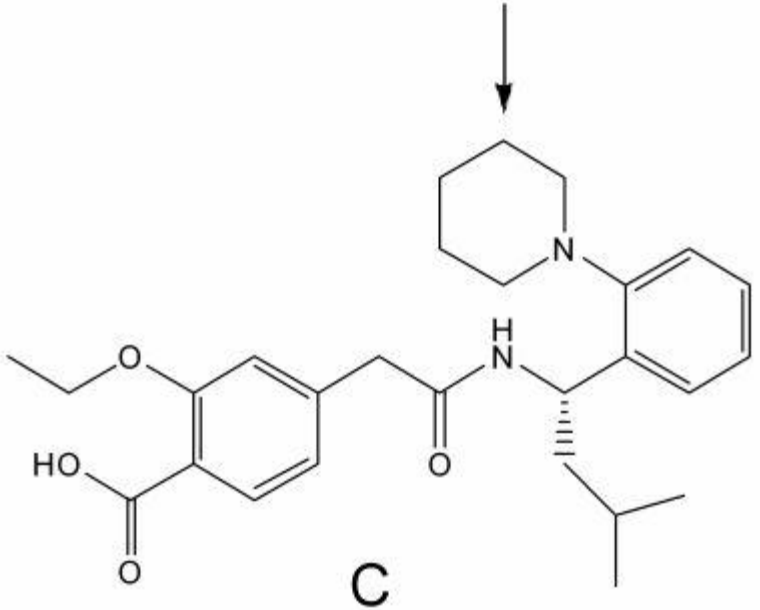

C

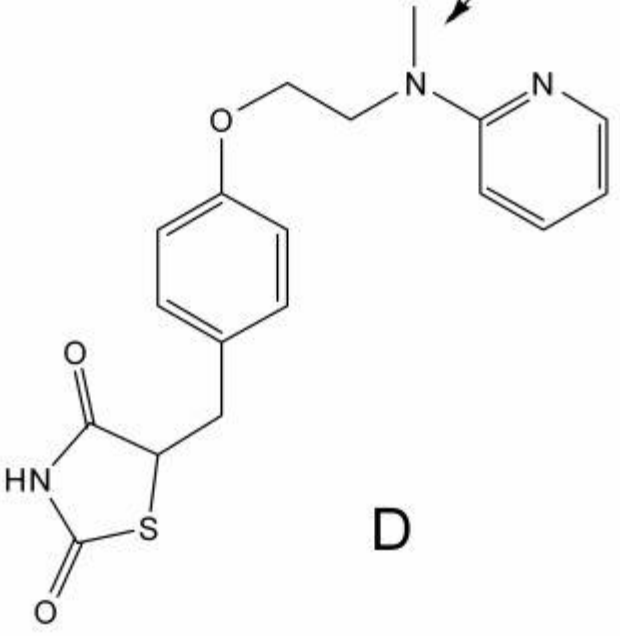

D

Figure 2

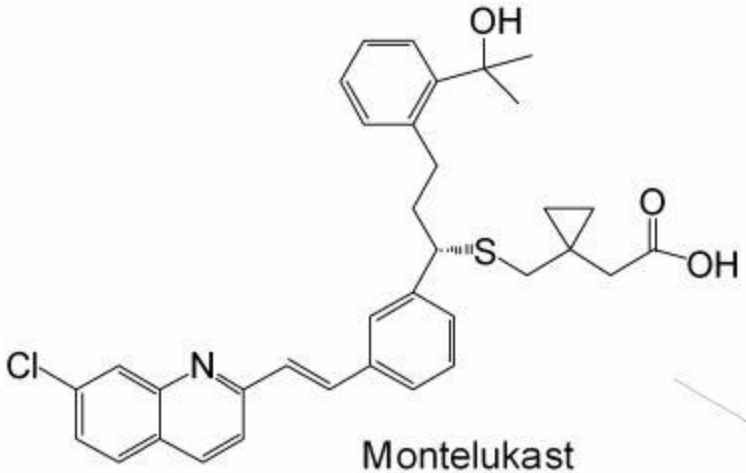

Montelukast

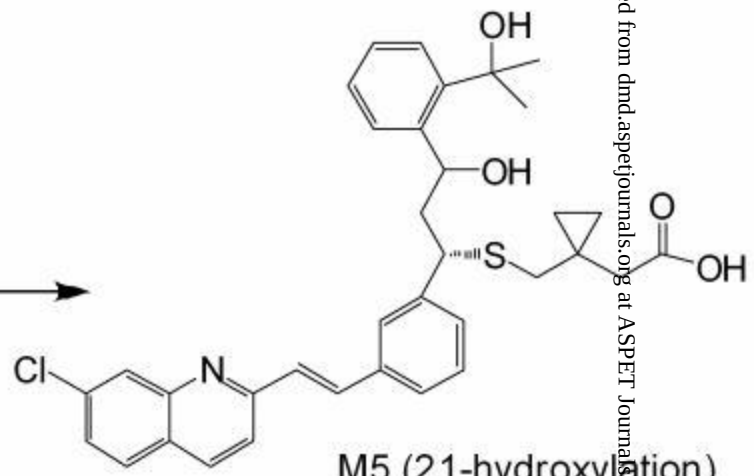

M5 (21-hydroxylation)

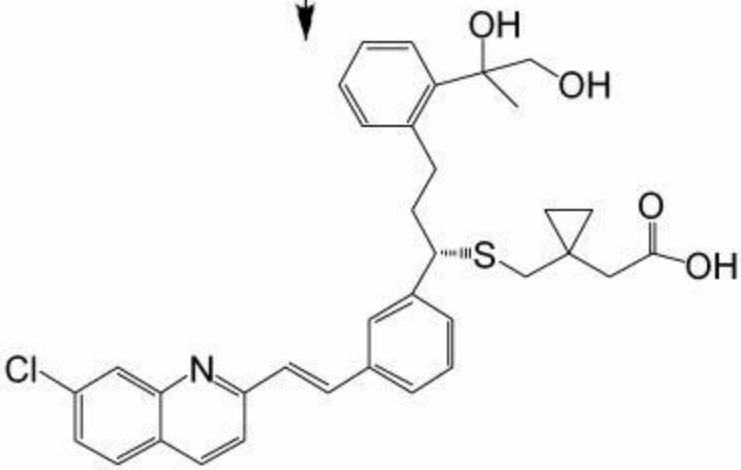

M6 (36-hydroxylation)

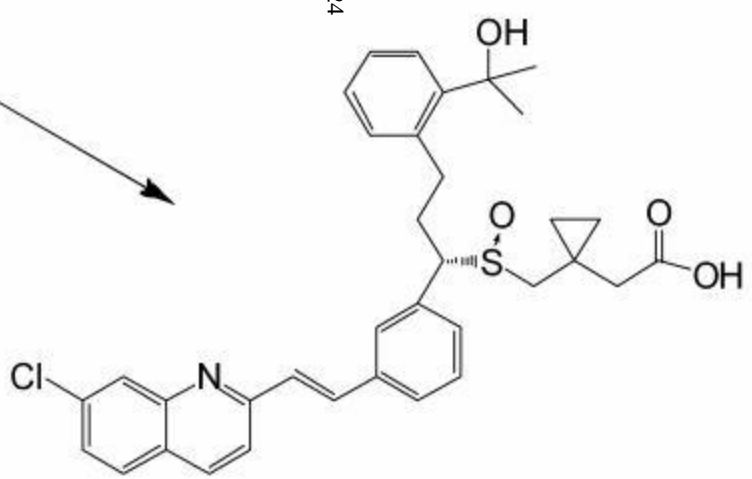

M2 (sulfoxidation)

Figure 3

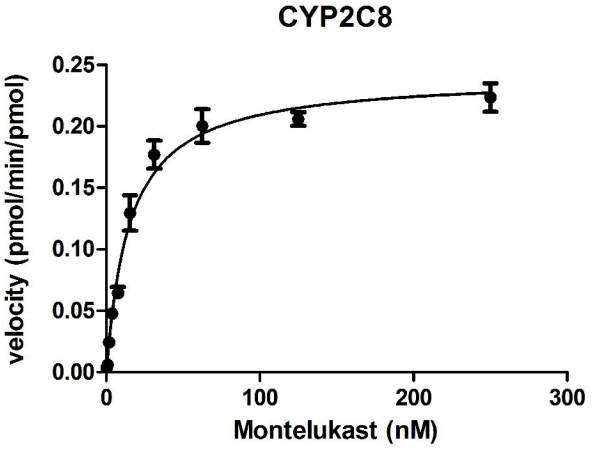
CYP2C8
velocity (pmol/min/pmol)
0.25
0.20
0.15
0.10
0.05
0.00
0
100
200
300
Montelukast (nM)

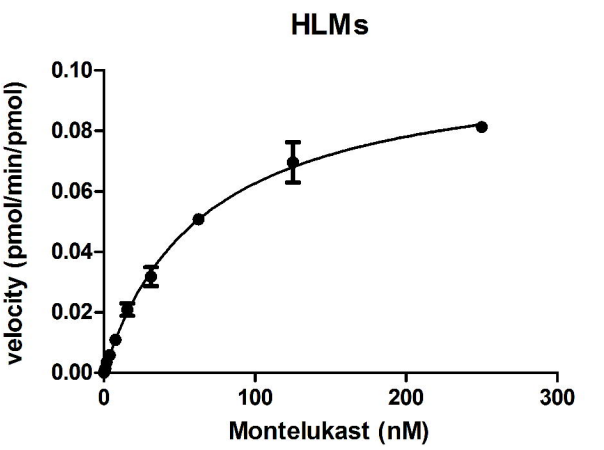
HLMs
velocity (pmol/min/pmol)
0.10
0.08
0.06
0.04
0.02
0.00
0
100
200
300
Montelukast (nM)

Figure 4

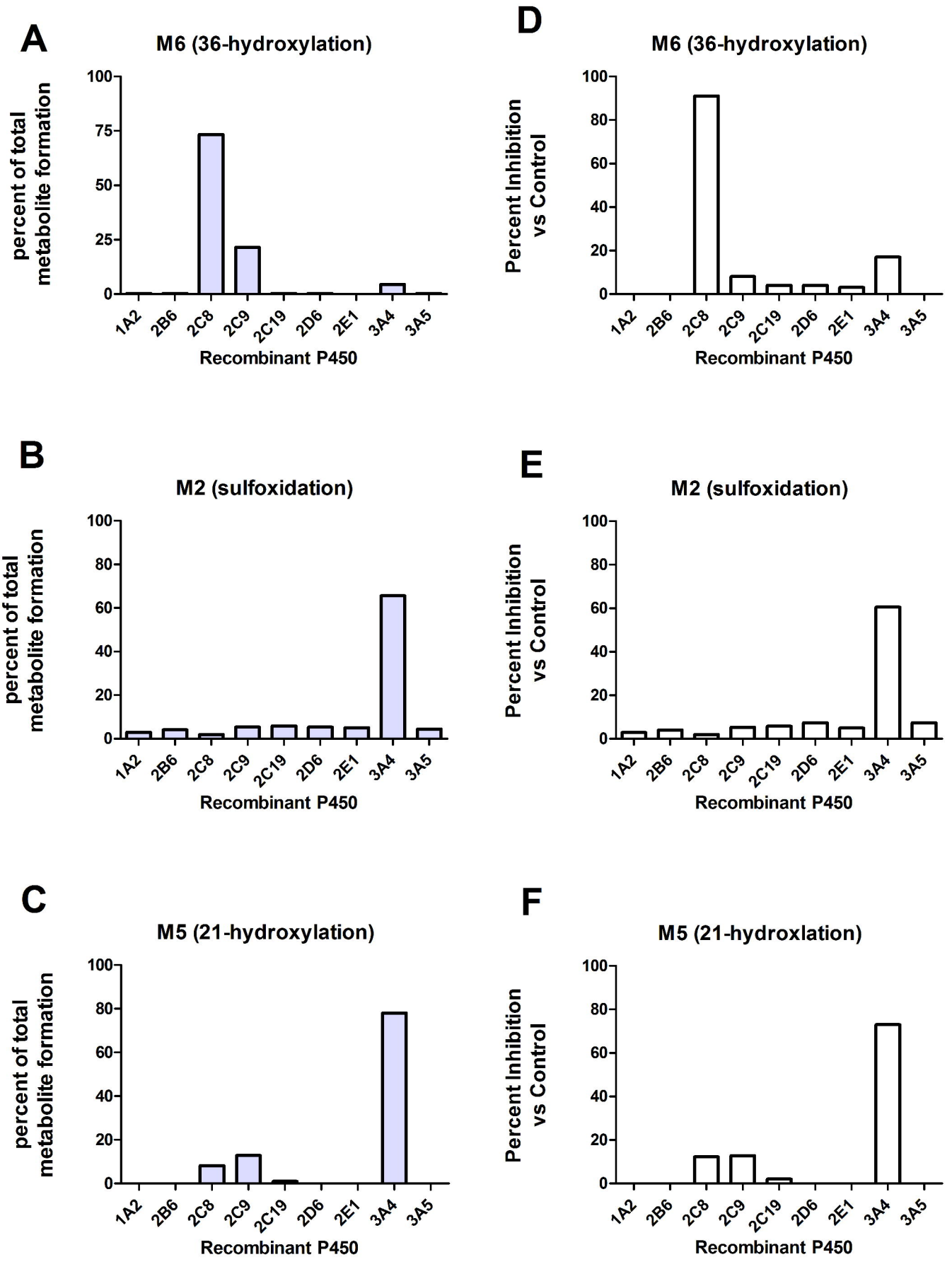
A
M6 (36-hydroxylation)
percent of total metabolite formation
100
75
50
25
0
1A2
2B6
2C8
2C9
2C19
2D6
2E1
3A4
3A5
Recombinant P450
D
M6 (36-hydroxylation)
Percent Inhibition vs Control
100
80
60
40
20
0
1A2
2B6
2C8
2C9
2C19
2D6
2E1
3A4
3A5
Recombinant P450
B
M2 (sulfoxidation)
percent of total metabolite formation
100
80
60
40
20
0
1A2
2B6
2C8
2C9
2C19
2D6
2E1
3A4
3A5
Recombinant P450
E
M2 (sulfoxidation)
Percent Inhibition vs Control
100
80
60
40
20
0
1A2
2B6
2C8
2C9
2C19
2D6
2E1
3A4
3A5
Recombinant P450
C
M5 (21-hydroxylation)
percent of total metabolite formation
100
80
60
40
20
0
1A2
2B6
2C8
2C9
2C19
2D6
2E1
3A4
3A5
Recombinant P450
F
M5 (21-hydroxlation)
Percent Inhibition vs Control
100
80
60
40
20
0
1A2
2B6
2C8
2C9
2C19
2D6
2E1
3A4
3A5
Recombinant P450

Figure 5

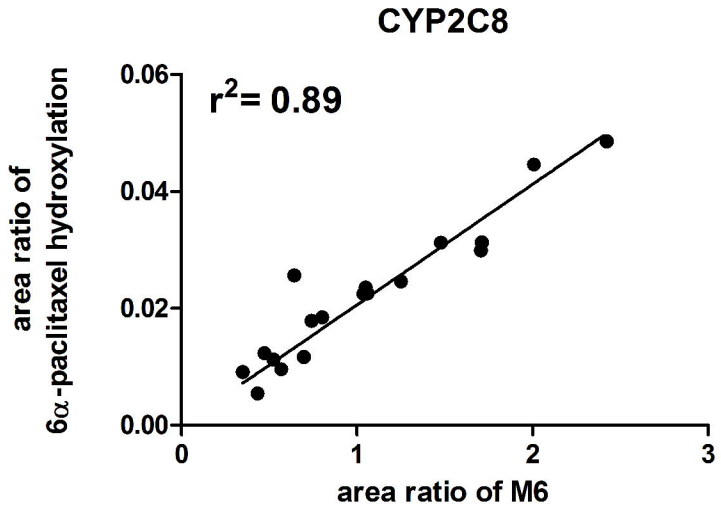
CYP2C8
r^2= 0.89
area ratio of 6α-paclitaxel hydroxylation
area ratio of M6
0.06
0.04
0.02
0.00
0
1
2
3

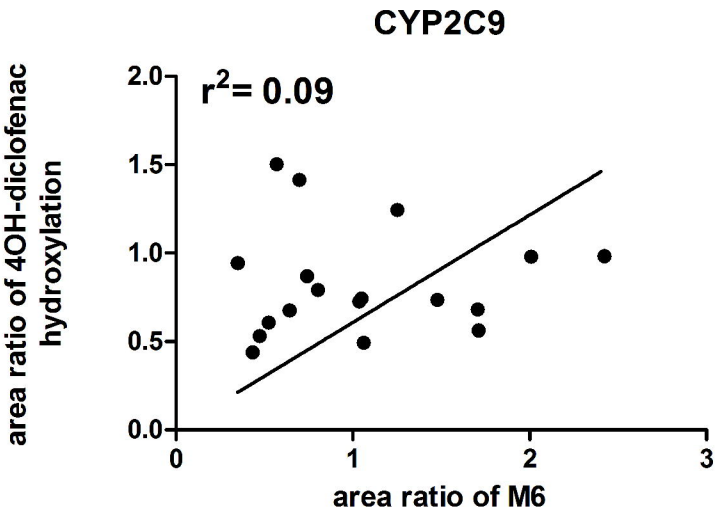
CYP2C9
r^2= 0.09
area ratio of 4OH-diclofenac hydroxylation
area ratio of M6
2.0
1.5
1.0
0.5
0.0
0
1
2
3

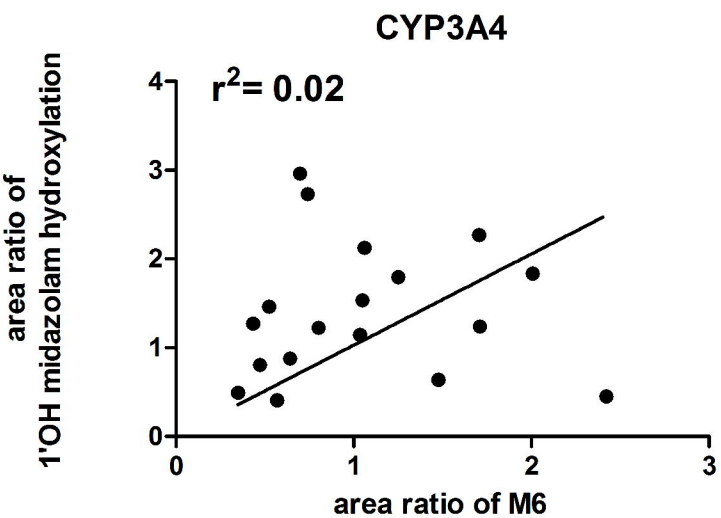
CYP3A4
r^2= 0.02
area ratio of 1'OH midazolam hydroxylation
area ratio of M6
4
3
2
1
0
0
1
2
3